

Formation of Metal Nanoclusters on Specific Surface Sites of Protein Molecules

Nathalie Braun¹, Winfried Meining², Ulrike Hars¹, Markus Fischer¹
Rudolf Ladenstein², Robert Huber³, Adelbert Bacher¹, Sevil Weinkauff^{1*}
and Luis Bachmann⁴

¹Department of Chemistry
Technical University Munich
Lichtenbergstr. 4, D-85748
Garching, Germany

²Karolinska Institutet
NOVUM, Center for
Structural Biochemistry
S-14157 Huddinge, Sweden

³Max-Planck-Institut für
Biochemie, Am Klopferspitz 18a
D-82152 Martinsried
Germany

⁴Institut für Physikalische
Chemie, Universität Innsbruck
Innrain 52a, A-6020 Innsbruck
Austria

During vacuum condensation of metals on frozen proteins, nanoclusters are preferentially formed at specific surface sites (decoration). Understanding the nature of metal/protein interaction is of interest for structure analysis and is also important in the fields of biocompatibility and sensor development. Studies on the interaction between metal and distinct areas on the protein which enhance or impede the probability for cluster formation require information on the structural details of the protein's surface underlying the metal clusters. On three enzyme complexes, lumazine synthase from *Bacillus subtilis*, proteasome from *Thermoplasma acidophilum* and GTP cyclohydrolase I from *Escherichia coli*, the decoration sites as determined by electron microscopy (EM) were correlated with their atomic surface structures as obtained by X-ray crystallography. In all three cases, decoration of the same protein results in different cluster distributions for gold and silver. Gold decorates surface areas consisting of polar but uncharged residues and with rough relief whereas silver clusters are preferentially formed on top of protein pores outlined by charged and hydrophilic residues and filled with frozen buffer under the experimental conditions. A common quality of both metals is that they strictly avoid condensation on hydrophobic sites lacking polar and charged residues. The results open ways to analyse the binding mechanism of nanoclusters to small specific sites on the surface of hydrated biomolecules by non-microscopic, physical-chemical methods. Understanding the mechanism may lead to advanced decoration techniques resulting in fewer background clusters. This would improve the analysis of single molecules with regard to their symmetries and their orientation in the adsorbed state and in precrystalline assemblies as well as facilitate the detection of point defects in crystals caused by misorientation or by impurities.

© 2002 Elsevier Science Ltd. All rights reserved

Keywords: nanoclusters; decoration; metal/protein interaction; electron microscopy; protein crystallization

*Corresponding author

Introduction

The formation of nanometer-sized clusters or islands is characteristic for the early stages of thin film growth during vacuum deposition of metals if the condensing atoms are more strongly bound to each other than to the substrate (Volmer–Weber mode).^{1–4}

Island formation requires the two-dimensional mobility of the condensing atoms. The adsorption energy is, in general, substantially larger than the activation energy of surface diffusion (referred to as “diffusion energy”). Therefore, it is possible for the adsorbed metal atoms to migrate over a wide area at proper substrate temperatures as long as re-evaporation is negligible. The average lifetime of an adatom at a certain site will be longer, the higher the diffusion energy at this site. During condensation of the metal on a perfectly uniform surface, the mobile adatoms of the metal will encounter other migrating adatoms or small

Abbreviations used: CM, centre of mass; EM, electron microscopy; PEG, polyethyleneglycol.

E-mail address of the corresponding author:
sevil.weinkauff@ch.tum.de

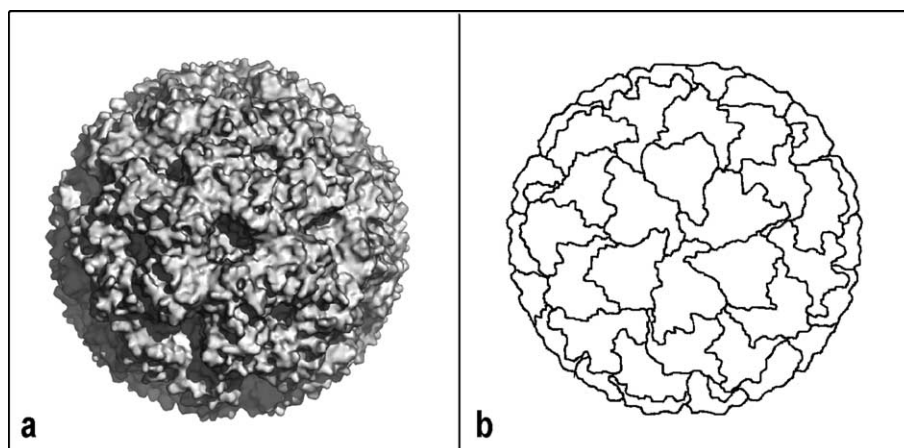


Figure 1. Lumazine synthase viewed along the 3-fold axis. (a) Relief; (b) arrangement of subunits.

clusters which will finally grow to stable and stationary islands at random positions. If, however, mobile atoms come across special sites which have higher adsorption and diffusion energies compared to the neighbouring places, these preferred sites will act as traps for the migrating adatoms and enhance the probability of stable cluster formation at these spots.

The condensation of noble metals on alkali halide crystals is one of the most explored systems where thin film formation follows the Völmer–Weber mode. In accordance with nucleation theories, electron micrographs of very thin deposits show linear cluster arrays, so-called “decoration lines”, besides randomly distributed metal islands. It was shown that decoration lines are caused by steps on the crystal surface which must be considered as linear arrays of special sites where preferred nucleation occurs.⁵ The average distance of the metal islands and even their size is several times as large as the lattice constants of the alkali halide and the number of clusters per area is only a fraction of the number of lattice points. Quantitative studies made it evident that not only steps but any local deviation from a perfect crystal surface, including point defects, may lead to structural differences of the deposit due to preferred nucleation on predetermined sites. Decoration has since been successfully applied to study growth mechanisms and surface defects on crystals by establishing affinity profiles of the substrate surface to the evaporated material.^{2,3,6}

The principles of thin film formation on inorganic substrates are also valid for metal condensation on protein molecules and their crystals. There are, however, different results obtainable by decoration if the size of the molecules is larger than the size of the metal clusters. Gold decoration patterns, obtained by averaging the metal distribution on protein membranes, have frequently revealed whether or not the molecules are packed in regular arrays.⁷ In this case, the number of clusters per area was comparable to the number of molecules. If the size of the molecules is con-

siderably larger than the average diffusion length of the condensing metal atoms, several clusters are formed on the surface of each molecule. On the surface of protein molecules, there are no areas of uniform affinity and the surface diffusion energy of the condensing metal fluctuates on an atomic scale. Thus, the “energy landscape” which the metal atoms encounter is very complex and the cluster positions on the surface of the macromolecules are always influenced by cluster formation on predetermined sites.

This paper deals with decoration of large enzyme complexes with molecular dimensions of 10–15 nm. This is considerably larger than the mean diffusion length of the metal in our experiments. Consequently, on each molecule several clusters are observed which form a decoration pattern characteristic for the kind of protein. The decoration patterns have already been used to determine molecular symmetries and the orientation of individual molecules which were either adsorbed to various substrates or arranged in crystal planes. Further applications included the determination of crystal packing and the analysis of crystal defects caused by misorientation of molecules or by inclusion of foreign molecules into the lattice.^{8–12}

Almost nothing is known about the nature of the special sites on protein surfaces and why they enhance or impede the probability of cluster formation. Understanding the influence of topochemistry on cluster formation might open the possibility to introduce more potent decoration sites as markers facilitating an improved analysis of symmetry and orientation of single protein molecules. Placing predominant decoration sites with high trapping efficacies onto selected areas of macromolecules may in turn open a possibility to generate designed patterns of supported nanoclusters with very high area densities and little background. The nanoparticles generated on proteins can be detached from these templates by evaporating a support film, e.g. of carbon or SiO₂, and floating the decoration replica on water.^{5,6,13}

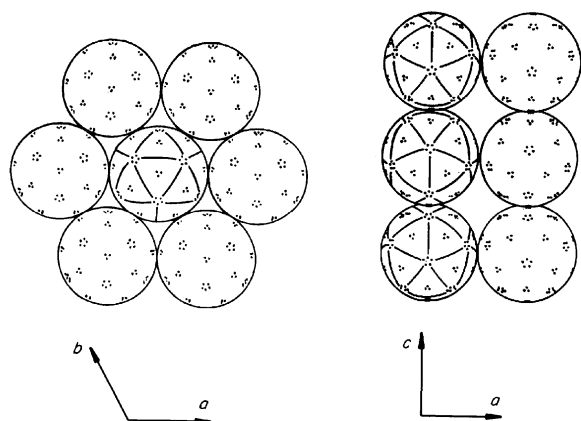


Figure 2. Crystallographic ab and ac planes of lumazine synthase; model based on X-ray data; space group $P6_322$. The molecules are shown as spheres with diameters equal to the lattice constants $a = b = 156.4 \text{ \AA}$. For demonstration of the icosahedral symmetry, each subunit is visualized by two points where the 3-fold and 5-fold axes penetrate the surface of the sphere.

The detailed correlation of the metal distribution with known atomic structures of the proteins might facilitate the application of non-microscopic physical-chemical techniques and even provide an experimental basis for theoretical studies on the interaction of metal atoms with biomacromolecules in their native state, a problem which is also of interest in the fields of biocompatibility and sensor devices.^{14–16}

Results

For a better understanding of the correlation of metal distributions on frozen-hydrated surfaces of the enzymes studied with their structures it is necessary to give some data on their morphology, symmetry and crystal packing.

Lumazine synthase/riboflavin synthase from *Bacillus subtilis*

Lumazine synthase/riboflavin synthase of *Bacillus subtilis* is a globular enzyme complex with a molecular mass of 10^6 Da (M_r) and a diameter of 15.6 nm . It consists of three α subunits (riboflavin synthase) enclosed by a capsid of 60 β subunits (lumazine synthase). The capsid has a spherical overall shape and $T1$ -icosahedral symmetry. At the areas of 3-fold and 5-fold symmetry the surface of the molecule has depressions of approximately 2 nm depth¹⁷ (Figures 1 and 5).

Hollow β_{60} capsids (lumazine synthase) have been reconstituted from isolated β subunits.¹⁸ Crystals of the native enzyme complex and the reconstituted hollow capsid, both referred to as LS, are isomorphous.⁹ The structure of the reconstituted capsid was determined at a resolution of 3.2 \AA ¹⁹ and of 2.4 \AA .²⁰ For primary structure see Ref. 19.

Both the $\alpha_3\beta_{60}$ and the β_{60} molecules crystallize in a modification with a hexagonal layer packing (space group $P6_322$; $a = b = 157.2 \text{ \AA}$, $c = 300.8 \text{ \AA}$, $\alpha = \beta = 90^\circ$, $\gamma = 120^\circ$) (Figure 2).

Proteasome from *Thermoplasma acidophilum*

The enzyme complex is composed of two different subunits α and β with molecular masses of 25.8 and 22.3 kDa , respectively. Seven identical subunits form rings with 7-fold symmetries. Four of these rings form a stack in which two β_7 rings are sandwiched between two α_7 rings. On negatively stained specimens the molecule appears barrel-shaped with a diameter of approximately 11 nm and a length of 15 nm .¹²

The structure of the proteasome was determined at 3.4 \AA resolution.²¹ Residues 1–12 do not show up on the electron density map and their positions are unknown. The analysed crystals belong to the orthorhombic space group $P2_12_12_1$ ($a = 311.9 \text{ \AA}$, $b = 209 \text{ \AA}$, $c = 117.2 \text{ \AA}$, $\alpha = \beta = \gamma = 90^\circ$) (Figure 3). The molecular 7-fold axis is inclined by 6.4° with respect to the crystallographic c -axis. For primary structure see Löwe *et al.*²¹

GTP cyclohydrolase I of *Escherichia coli*

The enzyme is a homodecamer with D_5 symmetry. Two pentamers are associated face to face forming a torus with a diameter of 100 \AA and a height of 65 \AA and with a central channel of approximately 10 \AA diameter at its entrance.

The monoclinic crystals of GTP cyclohydrolase I belong to the space group $P2_1$ ($a = 204.2 \text{ \AA}$, $b = 210.4 \text{ \AA}$, $c = 71.8 \text{ \AA}$, and $\alpha = \gamma = 90^\circ$, $\beta = 95.8^\circ$).²² The molecular structure at a resolution of 3 \AA was published by Nar *et al.*²³ The C-terminal residues 218–221 do not show up on the density map. The decoration patterns of the ab plane were published by Meining *et al.*¹⁰

Decoration patterns and the structural details on the underlying protein surfaces

The decoration patterns, i.e. the averaged metal distribution, were obtained by correlation averaging of the digitized micrographs. Decoration sites are special sites of distinct maxima or minima of the averaged metal thickness. Here, decoration patterns and electron micrographs are shown as photographic positives, i.e. metal appears dark.

Transmission electron micrographs contain quantitative information about the mass-thickness of the specimen. The optical transmission on the EM-negatives is proportional to the corresponding mass thickness up to $60 \mu\text{g/cm}$ for amorphous layers²⁴ and for microcrystalline deposits up to a cluster size of 5 nm .^{25,26} Therefore, in our studies, the local mass thickness at any site of the molecules surface can directly be determined from the EM-negatives as well as from the decoration patterns obtained by correlation averaging. The

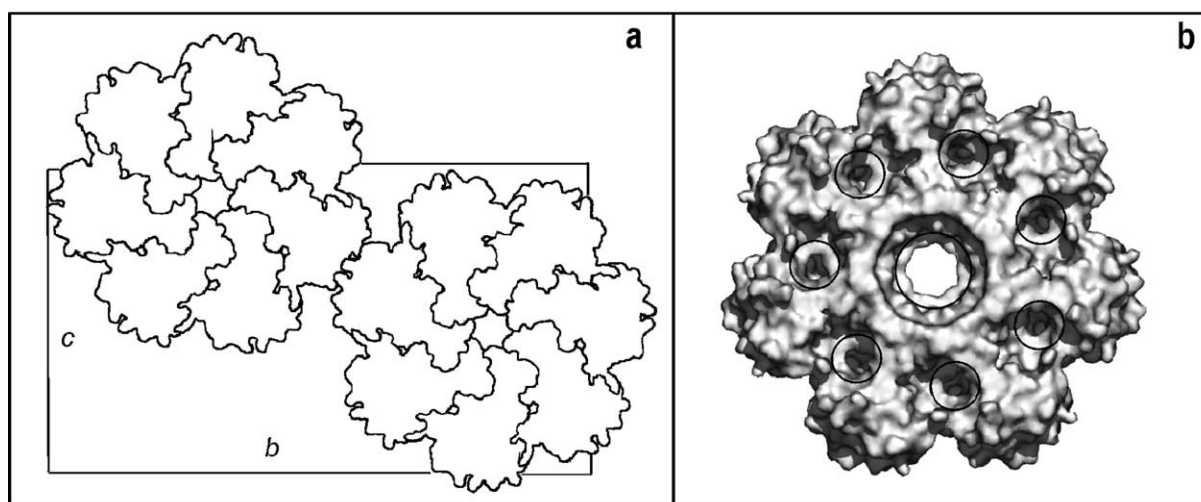


Figure 3. (a) The arrangement of proteasome molecules in the bc plane of the orthorhombic crystal (space group $P2_12_12_1$). Subunit borders are indicated. The α_7 rings are seen in front view. The neighbouring molecules are rotated with respect to each other by an angle of 25° . (b) Surface representation of the proteasome. The gold decoration sites (S_p) are indicated by circles.

accumulation coefficient $C_a = t_s/t_m$, i.e. the ratio of the local mass-thickness t_s on a site, an area or a pixel and the mean thickness of the metal deposit (t_m), is a measure of the relative efficacy of the many "competing sinks or traps"⁴ to accumulate the condensing metal. Accordingly, the accumulation contrast between two sites is the ratio of their accumulation coefficients. This kind of quantification of decoration patterns is strictly valid only if the flux of the evaporated metal is uniform over the specimen surface, thus requiring totally flat surfaces. Surface relief will introduce shadowing effects especially if the specimen is not oriented vertical to the direction of evaporation (Figures 4 and 7). When freeze-etched protein crystals are decorated, the crystal planes are neither totally flat because the molecules themselves have relief nor are the majority of the crystals in the frozen suspensions oriented exactly vertical to the evaporation source. Therefore, meaningful values of accumulation coefficients and accumulation contrast can only be obtained by analysing a large number of crystal planes with different degrees of shadowing and by preferentially comparing neighbouring sites with almost identical angles of metal incidence. The values obtained in this way are reproducible within $\pm 15\%$. The relative values between sites are estimated to be reproducible within $\pm 5\%$.

An alternative for measuring metal distribution is to analyse cluster positions.²⁷ This was done by determining the centre of mass (CM) for each metal particle on the micrograph. To each CM one pixel with a constant grey level was assigned and processed by correlation averaging. The resulting decoration pattern reflects the distribution of cluster densities (number of clusters per area) over the molecule's surface and is not influenced by the size, shape or mass of the individual clusters. In

analogy to the accumulation coefficient (C_a), which is a measure for the metal distribution, the cluster density coefficient (C_d) can be used to describe the spatial distribution of clusters in the averaged image. C_d is defined as the ratio of the cluster density at a particular site (d_s) to the overall cluster density (d_m): $C_d = d_s/d_m$. The corresponding cluster density contrast between two sites is the ratio of the cluster density coefficients of these sites.

The analysis of the cluster density distribution instead of the metal accumulation substantially reduces shadowing effects as demonstrated in Figures 4(c) and (d) and 7(c) and (d). While the position of the decoration sites remains the same, the maxima of the cluster positions are much better defined. This is demonstrated by the reduced half-width of the cluster density maxima compared with the metal distribution (Figures 4(e) and 6(e) and Tables 1 and 2). The results indicate that the positional fidelity of the clusters is neither sensitive to variations of the flux of the evaporated metals nor to the mean thickness of the deposits within the experimental variations of our studies (see Discussion).

Decoration of lumazine synthase of *Bacillus subtilis* (LS)

On electron micrographs of negatively stained single molecules of lumazine synthase (LS) and on Ta/W-shadowed freeze etched crystals the enzyme complex appears as a globular molecule without indications of surface relief or symmetry. Decoration replicas, however, readily reveal the icosahedral symmetry; even the poor decorating property of Pt/C proved to be sufficient. The hexagonal crystals of LS are particularly good objects for decoration studies aside from the appropriate size and symmetry of the molecule. Within an ab

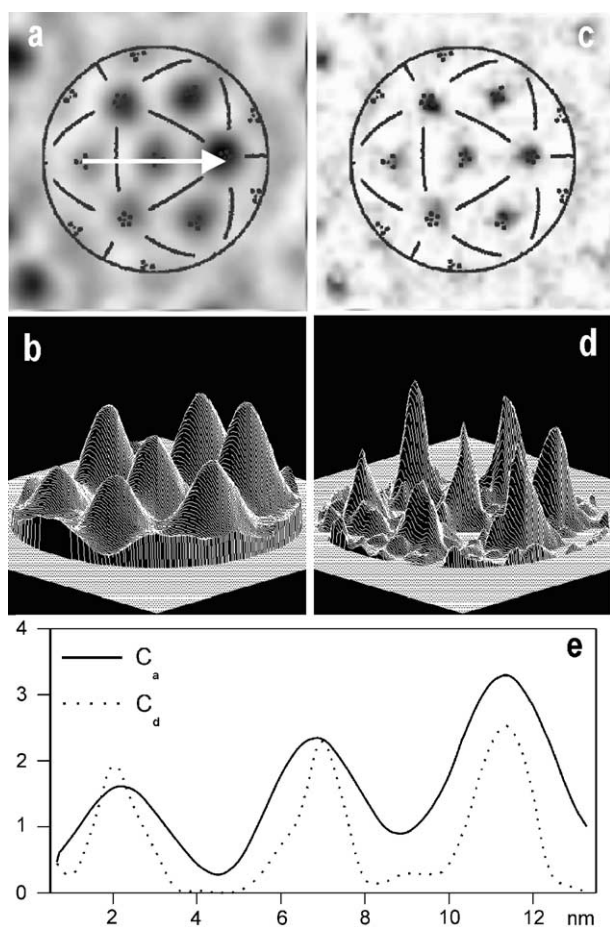


Figure 4. Decoration pattern of silver on lumazine synthase (0.4 nm silver; stabilized with 0.35 nm tantalum/tungsten). (a) Correlation average of metal distribution with an overlay of the spherical molecular model, direction of line scans in (e) indicated. (b) Three-dimensional representation of metal distribution. (c) Averaged spatial distribution of all clusters (centres of mass). (d) Three-dimensional representation of cluster distribution. (e) Line scans through the decoration patterns in (a) and (c); (—) accumulation coefficients C_a (normalised mass thickness); (···) cluster density coefficients C_d (normalised cluster density); width of the frames in (a)–(d), 20 nm.

plane, all molecules have the same orientation whereby 2-fold and 3-fold molecular and crystallographic axes coincide (Figure 2). Replicas of this crystal face are therefore easy to correlate with the molecular and crystallographic parameters. All decoration patterns on LS shown here were obtained from decorated *ab* crystal planes.

Decoration pattern of silver on LS

The decoration pattern (Figure 4) shows silver maxima which coincide with areas of 3-fold (S3) and of 5-fold (S5) symmetry on the surface of a spherical molecule with icosahedral symmetry. The overlay in Figure 4(a) and (c) is the computer-generated model of such a molecule in the orientation as in the *ab* plane (Figure 2). The areas of 2-fold symmetry (S2) are distinct metal minima (Figure 4). Accumulation coefficients and cluster density coefficients for S2, S3 and S5 are given in Table 1. The comparison of metal accumulation C_a and cluster density C_d at S2 suggests the presence of fewer clusters that are larger than on the other areas. This was verified by multivariate statistical analysis of S2 on individual molecules.

The metal and the cluster distribution can be influenced by chemical treatments of the molecules' surface. For example the heteropolytungstate complex $(\text{NaP}_5\text{W}_{30}\text{O}_{110})(\text{NH}_4)_{14}\cdot 31\text{H}_2\text{O}$ (WP) has 5-fold symmetry and was used for isomorphous replacement in X-ray crystallography. It binds preferentially to the sites of 5-fold symmetry on the surface of LS²⁸ (Figure 5). On the molecules treated with this compound, S5 is decorated much more strongly and by larger clusters than on S3.²⁷ The accumulation coefficients on S5 are increased relative to S3 raising the accumulation contrast S5/S3 from 1.3 to 1.9 (Table 1).

Surface structures of LS at areas of silver maxima S3 and S5

The overlay in Figure 4 illustrates that the silver maxima correspond to the 3-fold and 5-fold

Table 1. Accumulation coefficients (C_a), cluster-density coefficients (C_d) and decoration contrast for different sites on LS, LS/WP-derivative and proteasome

| A. LS native | | | | | | | | | | | |
|---------------|-------|-------|-------|-------|--------------------------|-------|--------------------------|-------|-----------------|-----------------|--|
| Metal | S5 | | S3 | | S2 | | Sg | | Contrast | | |
| | C_a | C_d | C_a | C_d | C_a | C_d | C_a | C_d | C_{a5}/C_{a3} | C_{d5}/C_{d3} | |
| Ag | 3.2 | 10 | 2.5 | 8.0 | 0.4 | <0.1 | 1.1 | 0.2 | 1.3 | 1.2 | |
| Au/Pd | 0.7 | 0.3 | 1.1 | 0.9 | 0.5 | 0.2 | 2.1 | 3.6 | – | – | |
| B. LS + WP | | | | | | | | | | | |
| Metal | S5 | | S3 | | S2 | | Sg | | Contrast | | |
| | C_a | C_d | C_a | C_d | C_a | C_d | C_a | C_d | C_{a5}/C_{a3} | C_{d5}/C_{d3} | |
| Ag | 3.0 | 6.6 | 1.6 | 3.2 | 0.7 | 0.2 | 1.1 | 0.6 | 1.9 | 2.1 | |
| C. Proteasome | | | | | | | | | | | |
| Metal | Sc | | Sp | | Minima between Sc and Sp | | Minima between Sp and Sp | | Contrast | | |
| | C_a | C_d | C_a | C_d | C_a | C_d | C_a | C_d | C_{ap}/C_{ac} | C_{dp}/C_{dc} | |
| Au | 2.6 | 2.8 | 2.3 | 3.6 | 0.6 | 0.6 | 0.3 | 0.3 | 0.9 | 1.3 | |

Table 2. Half-width values of averaged decoration maxima on LS and proteasome

| Protein | Decorating metal | Sites | Half-width (nm) of averaged decoration maxima | |
|------------|------------------|--------|---|----------------------|
| | | | Metal distribution | Cluster distribution |
| LS | Ag | S3, S5 | 2.5 | 1.3 |
| | Au/Pd | Sg | 1.3 | 1.1 |
| Proteasome | Au | Sp | 1.5 | 1.3 |
| | | Sc | 2.3 | 2.2 |

symmetry areas on the spherical model shown in Figure 2. The agreement between the decoration pattern and the spherical model which simplifies the protein surface according to X-ray structure (Figure 5) proves that the metal cannot be in direct contact with the protein on these sites and that the depressions must be filled with frozen buffer. The surface of these pores contains an abundance of charged and hydrophilic amino acid residues: at the site of trimer β -subunit contact (S3) there are

three lysine, three glutamate and nine serine residues and at the contact area of five β subunits (S5) there are ten lysine, five glutamate and five aspartate residues.¹⁷ The presence of these residues and the associated ions may lower the rate of sublimation sufficiently so that frozen buffer still remains there after freeze-etching. On WP-treated LS, where the pore at S5 is blocked by the WP complex, the clusters at position of S5 remain unaffected, which is an additional evidence for ice-filled pores on the untreated molecule.

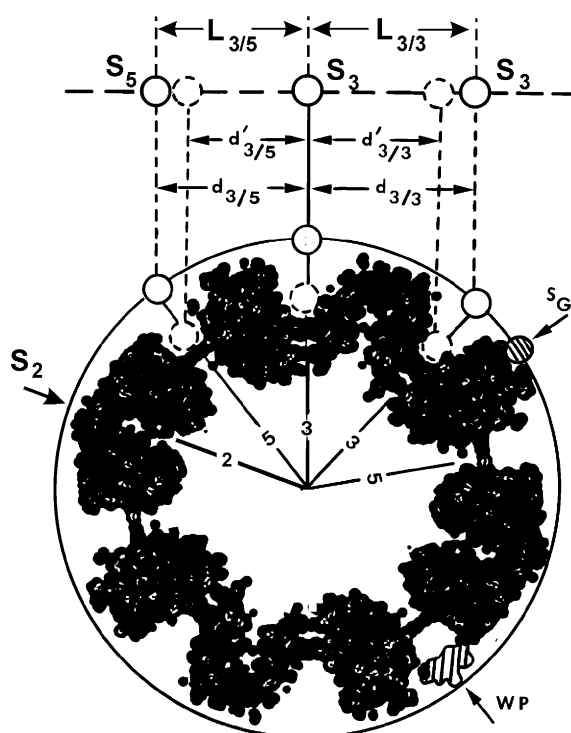


Figure 5. Cross-section through the space filling model of the β_{60} capsid of LS.¹⁷ Molecular symmetry axes lying in this sectional plane are indicated. The diameter of the circumscribed sphere corresponds to the lattice constant $a = b = 156.4$ Å. The observed silver decoration sites S3 and S5 are shown on top as filled circles, the respective distances S3/S5 and S3/S3 are designated L . Symmetry-related sites on the spherical model and on the true molecular envelope are also shown and their projected distances are indicated by d and d' , respectively. From the observed distances $d_{3/5}$ and $d_{3/3}$ on the decoration pattern, it follows that the silver clusters are not positioned in direct contact with the actual protein surface. The positions of one gold maximum (Sg), of one gold minimum (S2) and of one heteropolytungstate complex (WP) are indicated by arrows.

Decoration patterns of gold and gold/palladium on LS

In our experiments we found no significant differences in the decoration patterns of pure gold (99.99) and of gold/palladium (80/20). The strongest metal maxima (referred to as Sg) are located about halfway between S3 and S5 (Figures 5–7) with a slight counterclockwise offset between 0.2 and 0.6 nm from the direct line between S3 and S5 when viewed along a 3-fold axis from the outside of the molecule (Figures 5 and 6(a)). The gold site Sg is not located at a symmetry area. The shortest distance Sg/Sg is 3.1 nm. As in the case of silver decoration, the area of 2-fold symmetry S2 is also the minimum of the thickness and the cluster density of the gold deposit (Figures 5 and 7(e)). For quantitative data see Tables 1 and 2. The silver site is practically not decorated by gold.

The decoration pattern of gold is drastically changed on molecules treated with the heteropolytungstate complex WP (Figure 6(b)). S3 and S5 are even stronger decorated than Sg. The area connecting S3–Sg–S5 is also decorated, however, with a lower contrast. The pattern indicates that WP molecules act as special sites for gold and that they are not only present at S5 but also on other areas at low concentration and on less defined positions. S2 remains the absolute decoration minimum of metal deposition.

Surface structures of LS at area of gold maximum Sg

As the site of maximal gold accumulation Sg does not coincide with an area of molecular symmetry, its position cannot be given with the same precision as in the case of S3 and S5 but with an estimated maximal error of ± 3 Å. Figure 8 displays the protein surface underlying Sg. The

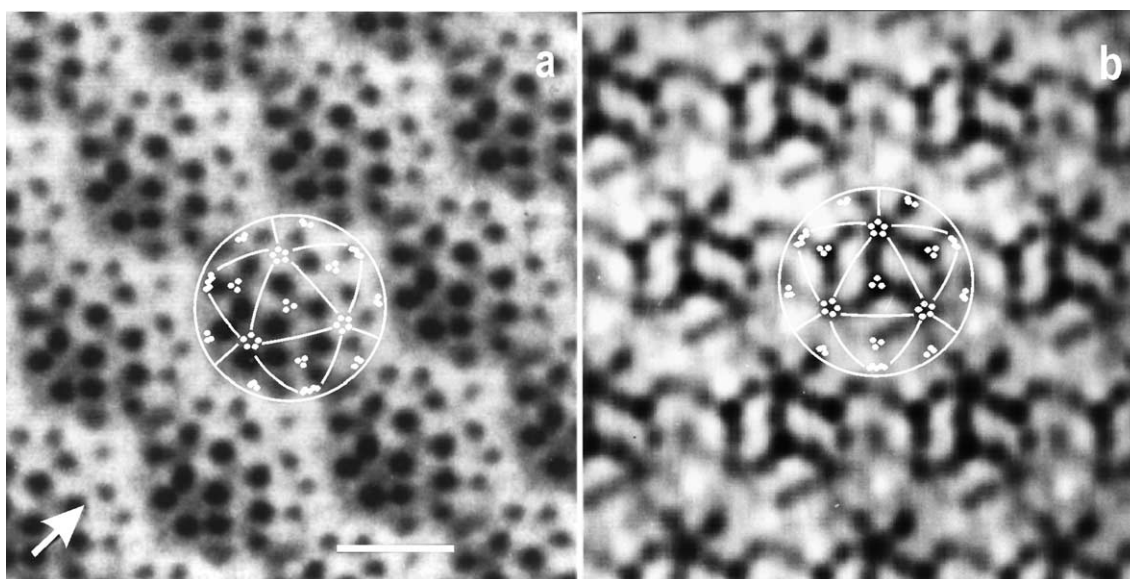


Figure 6. (a) Decoration pattern of gold/palladium (0.28 nm) on an *ab* plane of a LS crystal; arrow indicates direction of "shadowing"; bar represents 10 nm; (b) gold decoration of the WP derivative of an LS crystal, *ab* plane.

area is essentially formed by two overlapping subunits of the same pentamer. The result is a rather complex relief and topochemistry. The residues 1–9 and 145–154 of the subunit designated "O" cover parts of the subunit "U". The latter contributes to the surface with residues of the sequence segments 17–25, 48–54 and 62–72 (Figure 8). The main topographical feature of the area is the several Å high ridge along the border of the exposed parts of the subunits U and O. The centre of S_g is near a small area of subunit U which is exposed in a 2–3 Å wide corner or niche in the ridge at the subunit border. Within a few Å from the proposed centre two 2–3 Å wide gaps in the overlying amino acid residues Ile3 and Gln5 expose fractions of the residues Trp52 and Pro54 of subunit U. Within a circle of 1 nm diameter all residues are hydrophobic with the exception of Ser152. Outside this circle the polar groups of the following residues are located: Gln5, Lys65, Met66, Asp24 and the carboxy terminus of Glu154. The sulphur of Met1 is 1 nm away from the centre but not located on the surface (Figure 8). The charged polar groups of Lys64, Arg151 and Asn150 are outside the 2 nm diameter circle.

Protein surface at the 2-fold symmetry area of LS

Almost no clusters of silver or of gold are formed at the area of 2-fold symmetry S₂. In our opinion the protein structure of this area is as interesting as the structure at decoration maxima for a better understanding of decoration phenomena (Figure 9). S₂ is formed by the contact of two subunits from adjacent pentamers. When viewed along a 2-fold axis, within a circle of 2 nm diameter the outside surface of the capsid around S₂ is composed of sequence segments 7–13, 39–43 and 144–148, the last one being located more at the

periphery. Residues 130–143 are also located within the 2 nm circle around S₂, but they form the inner surface of the capsid and do not show up on the outer surface. The same holds for the residues 83–86 from two additional subunits. The residues closest to S₂ are the two His41 which form a narrow pore. The imidazole group of His41 is directed towards the inside of the capsid and is practically hidden from the outer surface. The other residues of the section 39–43 are hydrophobic with the exception of Arg40 whose amino groups are 8 Å away from the 2-fold axis and below the surface, hidden in part by Asn7. Residues 8–13 are hydrophobic with the exception of Thr11 and Asn7. Their polar groups are at the surface and their distance to S₂ is 4 Å and 7 Å, respectively. The carboxyl group of Glu145 is 8 Å away from the 2-fold axis below the surface hidden by Gly6 and Asn7. The polar group of Asn148 is at the surface 8 Å away from S₂.

In summary, within 10 Å from S₂ there are no charged groups at the surface and within 7 Å no polar groups except the two Thr11. Compared to S_g, S₃ and S₅ the relief at S₂ is relatively smooth.

Decoration of proteasome of *T. acidophilum*

Decoration pattern of gold on proteasome

The gold decoration pattern of the outer face of the α_7 -rings as exposed in a *bc* plane of an orthorhombic crystal is shown in Figure 10 and in more detail in Figure 11. Seven peripheral gold maxima (Sp) are located on a circle of 7 nm diameter around the central gold deposit (Sc) at the 7-fold symmetry area on the surface of the complex. The accumulation coefficients and the cluster density coefficients of Sc and Sp are included in Table 1. At the centre of the molecule (Sc), gold covers a

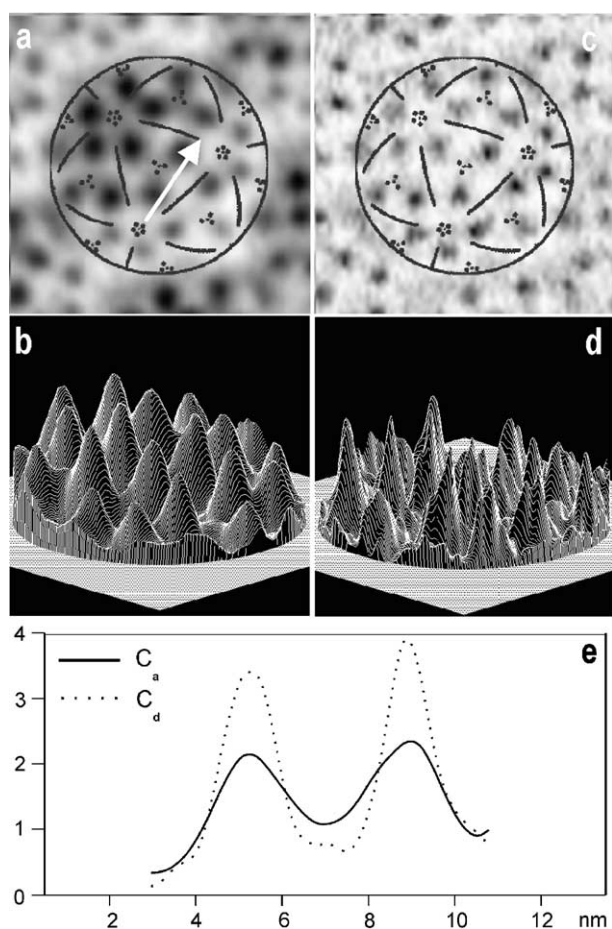


Figure 7. Decoration pattern of gold/palladium alloy 80/20 (0.28 nm) on an *ab* plane of a LS crystal. (a) Correlation average of metal distribution with an overlay of the molecular model, direction of line scans in (e) indicated. (b) Three-dimensional representation of metal distribution. (c) Averaged spatial distribution of all clusters (centres of mass). (d) Three-dimensional representation of cluster distribution. (e) Line scans through the decoration patterns in (a) and (c); (—) accumulation coefficients C_a (normalised mass thickness); (···) cluster density coefficients C_d (normalised cluster density); width of the frames in (a)–(d), 21 nm.

larger area than at the peripheral Sp site and the clusters are larger. Cluster density analysis on Sc did not significantly improve the sharpness of this site (Figure 11(b)). The half-width of the cluster density distribution at Sc is 2.2 nm, which is 1.7 times larger than the value at Sp, indicating a poor positional fidelity of the clusters at Sc (Table 2, Figure 11(e)). The average size of the gold clusters at Sc is 1.4 times larger than the clusters at Sp. Figure 11(c) and (d) demonstrates the effect of separately averaging of clusters of different size.

Structure of proteasome at the gold site Sc

Along the 7-fold molecular axis the barrel-shaped molecule has a central channel penetrating the molecule (Figures 3(b) and 12(b)). The amino acid residues Tyr126, Gly127 and Gly128 of the

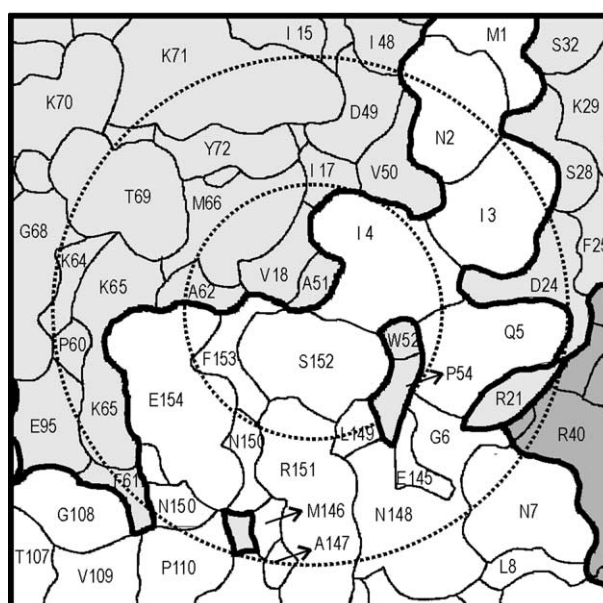


Figure 8. (a) The amino acid residues according to X-ray structure analysis²⁰ located on the surface of LS underlying the gold decoration maximum Sg. The residues of the sequence segments 1–9 and 145–154 of the overlying subunit O are shown in white, the segments 17–25, 48–54 and 62–72 of the underlying subunit U are shown in light grey. Amino acid residues of a third subunit on the right lower area are dark grey. The diameter of the inner circle is 1 nm, of the outer circle 2 nm.

α -subunits form a hydrophobic ring leaving only a passage of 1.3 nm diameter at the entrance.²¹ This ring-shaped plateau is lower than the surrounding surface forming a depression with a

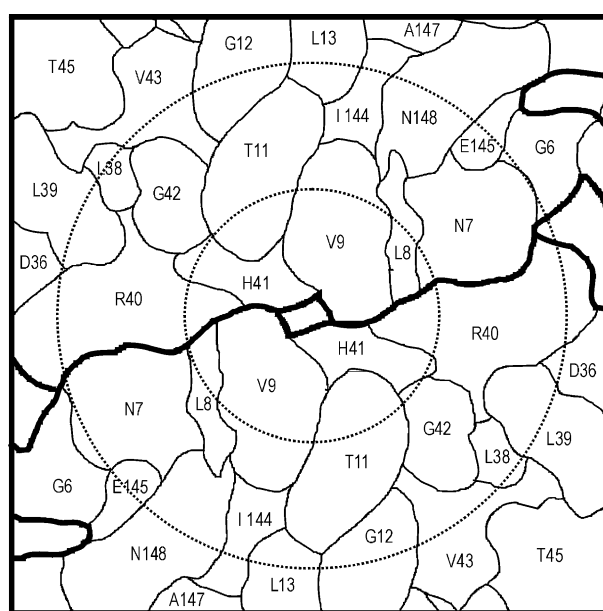


Figure 9. The amino acid residues located on the surface of LS underlying the symmetry area S2 according to X-ray structure analysis.²⁰ Diameter of the circles 1 nm and 2 nm, respectively.

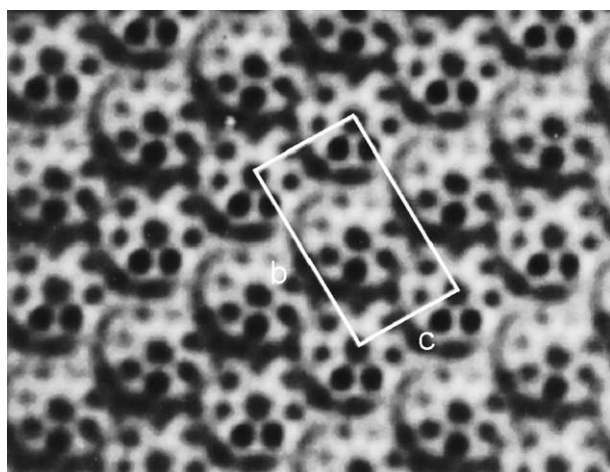


Figure 10. Decoration pattern of gold on a bc plane of a proteasome crystal with the molecules in end-on orientation (front view). The two-dimensional unit cell bc (lattice constants $b = 209 \text{ \AA}$, $c = 117.2 \text{ \AA}$) is indicated.

diameter of 2–2.5 nm and a depth of 1–1.5 nm (Figures 3(b) and 12(b)). The amino-terminal residues 1–12 are not visible on the electron density map and their location is uncertain. After freeze-etching, the channel and possibly even parts of the surrounding depression will remain filled with frozen buffer. In this case, nucleation of the gold clusters at Sc will occur over a larger area and not in direct contact with amino acids on fixed positions but on frozen buffer which may contain some of the residues 1–12 with unknown positions. Nucleation over a large area would be in accordance with the observed large half-width of the metal distribution and of the cluster density distribution (Figure 11(e) and Table 2).

Structure of the proteasome at the gold site Sp

The peripheral gold site Sp is located in a surface depression and close to an approximately 0.3 nm wide pore or channel at the border of two α -subunits of the homo-heptamer (Figure 12(b)). The approximately 1 nm deep depression is surrounded by the higher regions of residues 19–20 and the helix H0 (21–32) of one subunit and by the β -sheet S2 and the loop region S3 (50–66) of the neighbouring subunit.²¹

The amino acid residues that are exposed on the surface are shown in Figure 12(a). The centre of the gold site is located on the exposed part of Asn158 of the β -sheet S7 which is adjacent to the pore. Parts of the residues Asp150, Thr156, Ile157, Glu159, Tyr160 and very small parts of Lys114 and Arg147 of the same subunit appear as next neighbours to Asn158 on the surface. Ile59, Ser63, Ile64 and Glu65 of the adjacent subunit are also located within a 1 nm circle around Sp. Within a 2 nm diameter circle the following additional residues are located: Arg28, Lys33, Ile137, Cys151, Asp152, Val173, Asp170 and from the neighbour-

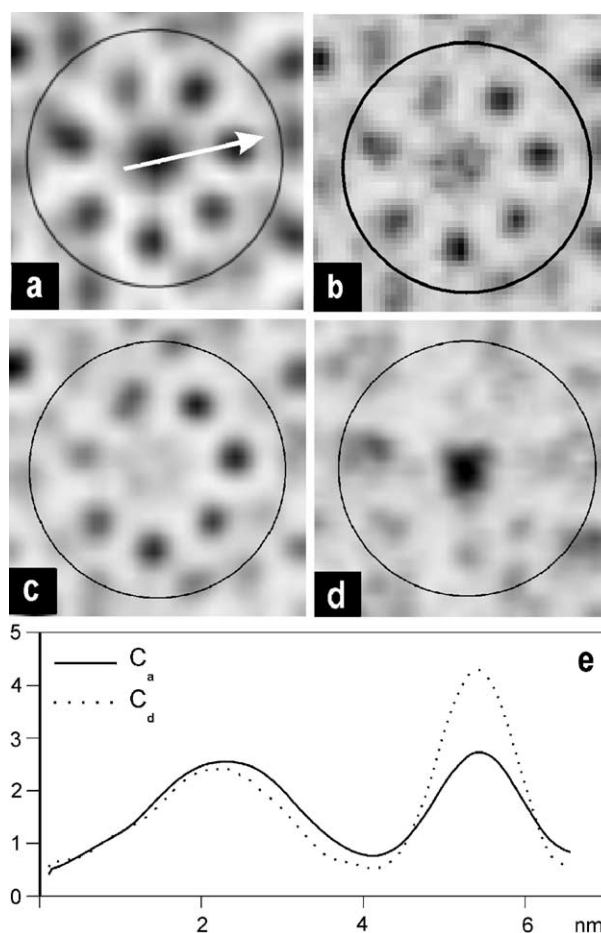


Figure 11. Decoration pattern of gold (0.2 nm) on proteasome in end-on view obtained by correlation averaging of a bc plane. (a) Correlation average of metal distribution, direction of line scans in (e) indicated. (b) Centre of mass average of all clusters. (c) Centre of mass average of small clusters (\varnothing 0.5–1 nm). (d) Centre of mass average of large clusters (\varnothing 1.5–2.5 nm). (e) Line scans through the decoration patterns in (a) and (b); (—) accumulation coefficients C_a (normalised mass thickness); (\cdots) cluster density coefficients C_d (normalised cluster density); width of the frames in (a)–(d), 15 nm.

ing subunit Lys52, Lys53, Val54, Arg55, Ser56, Leu58, Gln68, Val82, Ala83, Arg86 and Arg93. The polar group of Asn158 is fully exposed on the surface, Glu159 is oriented downward and the carboxyl group is partially hidden. The phenoxyl group of Tyr160 is pointing upward towards the surface. The amino group of Lys114 is about 1 nm below the surface level. The amino groups of Arg55 are right at the surface, the polar group of Gln68 is at the edge of the 2 nm area.

Decoration pattern of silver on proteasome

Only the central 7-fold area Sc is strongly decorated. A weak and vaguely defined silver site can be noticed at the fringe of the molecule some 20 \AA further away from the centre than Sp of gold.

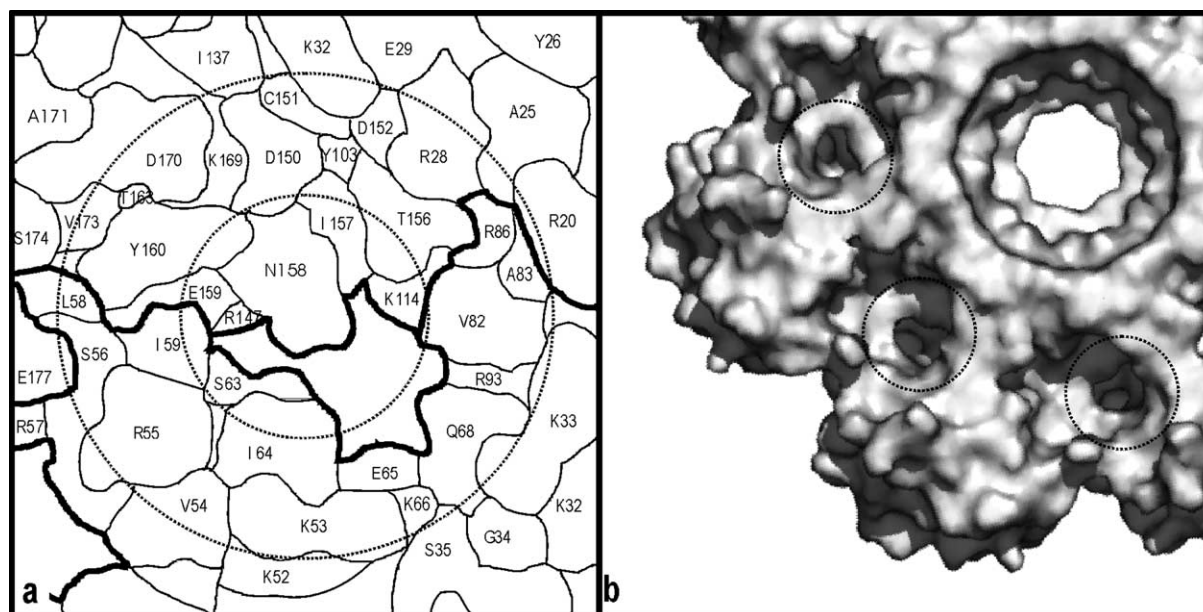


Figure 12. (a) The amino acid residues located on the surface of proteasome underlying the gold decoration maximum Sp according to X-ray structure analysis.²¹ The diameter of the circles is 1 nm and 2 nm, respectively. (b) Relief representation of the proteasome. The gold decoration sites Sp are indicated.

Decoration of GTP cyclohydrolase I of *E. coli*

Decoration pattern of silver on GTP cyclohydrolase I

Silver decorates the central area on the surface of the molecule. Rotational correlation analysis of the deposit at the centre revealed a 5-fold symmetry.¹⁰

Decoration pattern of gold on GTP cyclohydrolase I

Gold accumulates in a ring-shaped arrangement of five maximas around the central area on the molecule's surface. The distance of the molecule's centre to the gold maxima is approximately 20 Å. The centre of the molecule is not decorated.¹⁰

Structure of GTP cyclohydrolase I at decoration sites

The central cavity of the torus is occupied by the C-terminal region. The C terminus consisting of the charged Arg218, His219, His220 and the polar Asn221 are disordered and do not show up on the electron density map.²³ It is reasonable to assume that at freeze-etching conditions the central cavity with an opening of approximately 15 Å diameter remains filled with frozen buffer.

A correlation of the gold decoration site with the protein structure is not yet available with sufficient accuracy to determine the underlying amino acid residues. The positions of gold clusters correspond to an area with very rough relief.

Discussion

This paper correlates decoration patterns of gold and silver with the underlying structure of the protein surface as determined by X-ray analysis. In our experiments, the surface under investigation is obtained by freezing the suspension of protein crystals in growth medium. The relatively low cooling rate of approximately 100 K/second results in an almost complete segregation of pure ice and the solute. This way, large areas of the protein crystals become embedded in pure ice. After exposing the protein surface by vacuum sublimation of ice at 170 K, high resolution replicas of these areas reveal the protein molecules of the apparently "clean" crystal surface. Some of the ingredients of the suspension medium (buffer, substrate analogue, sodium azide, etc.), however, may still remain attached to the protein surface during the freezing process and would not be removed by the subsequent sublimation of ice. In this case, the decorating material will not always directly interact with the bare X-ray structure of the hydrated protein but with a surface modified by low molecular weight compounds which are bound to specific sites of the protein. Considering these points, it is not known to what extent the energy landscape as obtained by freeze-etching deviates from the surface revealed by X-ray structure analysis.

Aside from the question to which extent the ingredients from the mother liquor affect the decoration, the results raise other and more specific questions on the strikingly different behaviour of gold and silver. These metals prefer entirely different sites for cluster formation, for instance on LS, either native or after chemical treatment with WP. On the native enzyme, silver decorates only the

pores at the sites S3 and S5 which are filled with frozen buffer. These sites, however, are practically not decorated by gold. On the other hand, both silver and gold strictly avoid condensation on another specific site (S2) of the native and of the WP-treated molecule. Actually this minimum of metal thickness at the 2-fold symmetry area is one of the most constant decoration features on LS.

On GTP cyclohydrolase I, silver also decorates the central channel of the enzyme presumably filled with frozen buffer while gold does not decorate this area.^{10,23} It should be noted that the crystals of LS and GTP cyclohydrolase I are frozen in different buffers: LS in phosphate, GTP cyclohydrolase I in citrate.

On proteasome, silver again decorates practically only the central channel Sc filled with frozen buffer and in this respect similar to the silver sites S3 and S5 on LS. On proteasome, however, the frozen-buffer area Sc is also a decoration site for gold and this central channel is filled with phosphate buffer with the addition of 10% polyethylene glycol and possibly with some of the 12 amino-terminal residues with unknown positions.

On all three enzymes, there are sites that are decorated with gold but not with silver. A comparison of the protein structure at gold sites Sg on LS and Sp on proteasome indicates only vague similarities. Both areas have a rough relief: Sp is located within a wide depression near a small pore while Sg is at an almost 10 Å high edge of two overlapping subunits. In both cases a polar but uncharged residue is at or very close to the decoration centre, surrounded by hydrophobic residues. On GTP cyclohydrolase I, the gold clusters are also formed on areas of rough relief.

At the site S2 on LS, identical sections of two subunits are attached to each other in antiparallel orientation. The relief is less rough than at Sg and Sp. Within a diameter of 7 Å only two polar residues are located (Thr11). There are no charged residues within a 10 Å diameter area if the two central His41 are disregarded, whose imidazole groups are hidden deep below the surface.

Decoration cannot be compared with chemical staining where a given compound binds to certain reactive groups wherever they are accessible. If these chemical groups are absent, no staining occurs. Under the experimental conditions of this study the evaporated metal must condense somewhere on the substrate because of the high supersaturation. Cluster formation at preferred sites is governed by the kinetics of thin film formation. Therefore, decoration of a specific site cannot be fully understood by analysis of the trapping energy and the structure of this site only. It is the lower level of diffusion energies and thus of the shorter life times of the adatoms at the competing sites in the surrounding energy landscape which makes the decoration site efficient. On inorganic crystals, such as alkali halides and magnesium oxide, the diffusion and binding energies at different sites and for different metals have been

measured by analysing the deposits of these metals obtained at different deposition rates and substrate temperatures.³ Similar measurements on hydrated protein surfaces could not be performed without considerable experimental efforts to prevent alterations of the substrate properties and post-deposition changes of the metal distribution. Therefore, only the overall diffusion energy of metals on frozen proteins can be estimated.

On homogeneous surfaces, the number of clusters per area (cluster density) increases up to a certain thickness range of the deposit. This maximum of cluster density remains fairly constant throughout a range of increasing thickness before the density drops again due to island coalescence. The maximum density is therefore also referred to as saturation density. At sufficiently low temperatures where re-evaporation is negligible, the level of the density plateau depends primarily on the deposition rate, the diffusion energy of the metal and the substrate temperature.

On heterogeneous surfaces, such as proteins, cluster density also reaches a saturation plateau. The saturation density, however, is to a large degree independent of the deposition rate but corresponds primarily to the density of the dominating traps for the particular model.²⁹ At saturation density, the quality of the decoration pattern can be influenced by variation of the substrate temperature. At low temperatures, even sites with low diffusion energies contribute substantially to cluster formation while at higher temperatures only sites with high diffusion energies remain efficient traps. In our decoration experiments, the local deposition rate and mean film thickness varies on one and the same molecule due to the spherical shape of the molecule and, most frequently, to an even higher degree due to the non-vertical incidence of the evaporated metal (shadowing effect). On the averaged cluster densities, the shadowing effects on the decoration patterns are diminished compared to the averages of metal distribution (Figures 4(c) and 7(c)). This proves that density and position of the clusters reflect to a large degree the position and density of the special sites and that the cluster density on the replica corresponds to the saturation plateau. Still, the decoration patterns are far from ideal. Quantitative analysis of density and position of clusters on the individual molecules of a LS crystal plane decorated with silver indicated that 70% of the clusters are located at the decoration maxima S3 and S5. The remaining 30% appear as background on the averaged decoration pattern. It is not known, whether these clusters are formed on less efficient traps inherent to the protein surface or on randomly distributed remnants of the buffer solution or impurities. The analysis has further shown that the probability of more decoration sites on a LS molecule being occupied by metal clusters approximates a binomial distribution. It was found that on 85% of the molecules, four or more of the seven sites in the central part of the two-dimensional projection of the molecule are occupied.^{27,30}

Optimal patterns of nanoclusters with little background could be obtained by deposition of the metal at conditions of cluster density saturation on a substrate consisting of very efficient trapping sites which form a pattern on an otherwise homogeneous surface. Homogeneous areas, however, do not exist on proteins. Therefore, the desired special sites (pattern forming traps) must be strong enough and sufficiently close to each other as to impede stochastic cluster formation on competing weaker sites on the energy landscape in between. Their distance, however, has to be large enough not to compete with each other and thus all desired sites are occupied by clusters. Understanding the interaction of metal and protein surfaces would help to design such efficient trapping sites. This interaction has an influence on the electronic state of the metal as well as on the fine structure of the involved sections of the substrate molecule. These effects can be investigated by various physical-chemical techniques as used in the field of heterogeneous catalysis. For a detailed characterization of trapping sites, methods of surface spectroscopy may be applied. These techniques do not depend on ordered arrays or crystals of macromolecules; adsorbed layers are sufficient. Electronic interaction of a gold substrate with adsorbed protein has been investigated by spectroscopic ellipsometry.^{14,15} The present study has shown that the positions of the most efficient trapping sites can be correlated with the surface structure within a nanometer. This localization of the metal/protein contacts should substantially facilitate the interpretation of the spectroscopic data. Our experiments have further shown that the energy landscape of a protein can be altered by attaching dominant trapping sites onto the surface *via* chemisorption of small molecules or ions. Treatment of LS with the polytungstate complex WP leads to specific changes of the metal distribution for silver and gold as well as to changes of the cluster density distribution and of the cluster size distribution. Decoration of proteins with sequence variations, either stemming from different organisms or modified by genetic engineering, would be an alternative to decoration of chemically treated molecules and may provide additional insights into the mechanism of decoration.

Materials and Methods

Proteins

Lumazine synthase/riboflavin synthase complex of *B. subtilis* and reconstituted lumazine synthase were purified and crystallized by published procedures.^{9,11,18,31} Batch crystallisation in phosphate buffer was preferred to obtain crystals of approximately 20 μm size which are optimal for freeze-etching.⁹

Proteasome from the archaeobacterium *T. acidophilum* was purified and crystallized in a mixture of phosphate buffer and polyethyleneglycol (PEG) as described.¹²

GTP cyclohydrolase I from *E. coli* was prepared and crystallized in citrate buffer according to published procedures.²²

Specimen preparation, electron microscopy and image analysis

Suspensions of protein crystals were frozen in liquid nitrogen in their growth medium. Due to the quasi-eutectic separation of ice and buffer during freezing, it is possible to expose molecular surfaces of the crystals by sublimation of ice at 173 K in a freeze-etching apparatus (BA360 or BAT 400T) for one to two minutes. Under these conditions only unbound, free water evaporates and the protein remains in the frozen-hydrated state. The decorating materials silver, gold and gold/palladium (80/20) were deposited at 165 K at 90° incidence. The thickness of the deposits varied between 0.5 and 2.5 monolayers (1–5 Å). In order to reduce cluster coalescence on silver-decorated replicas during storage at room atmosphere, a thin layer of Ta/W was evaporated onto the silver layer. After coating the specimen with a carbon layer, the replica with the attached metal clusters was floated on water and transferred on specimen grids for observation in the electron microscope. More experimental details have been published.^{27,32,33} Electron micrographs were taken at 33,000 and 50,000 magnification on a JEOL 100 CX.

For image analysis, the micrographs were digitized with a pixel size corresponding to 0.45 or 0.3 nm on the specimen level. Correlation averaging without imposing any symmetry³⁴ was performed using the SEMPER software package. For the analysis of particle orientation and of the cluster distribution of individual molecules in a crystal lattice, multivariate statistical analysis³⁵ was applied. The orientation of adsorbed individual molecules was analysed by model comparison.¹¹ All electron micrographs and decoration patterns obtained by image analysis are shown as positives. Surface modeling was done using INSIGHT, the position of the residues was determined using the program O.³⁶

Acknowledgments

This work was supported by grants from the Deutsche Forschungsgemeinschaft, the German Space Agency (D.L.R.) and the Fonds der Chemischen Industrie. We thank Dr G. Richter and F. Wendling for help with molecular graphics.

References

1. Bauer, E. (1958). Phenomenal theory of precipitation on surfaces. *Z. Kristallogr.* **110**, 395–431.
2. Lewis, B. & Anderson, J. C. (1978). *Nucleation and Growth of Thin Films*, Academic Press, New York.
3. Venables, J. A. (2000). *Introduction to Surface and Thin Film Processes*, Cambridge University Press, Cambridge, UK.
4. Zhang, Z. & Lagally, M. G. (1997). Atomistic processes in the early stages of thin film growth. *Science*, **76**, 377–383.
5. Bassett, G. A. (1958). A new technique for decoration of cleavage and slip steps on ionic crystal surfaces. *Phil. Mag. Ser.* **83**, 1042–1045.
6. Bethge, H., Krohn, M. & Stenzel, H. (1987). Indirect imaging of surfaces by replica and decoration techniques. In *Electron Microscopy in Solid State Physics*

- (Bethge, H. & Heydenreich, J., eds), pp. 202–218, Elsevier, Amsterdam.
- Neugebauer, D.-Ch., Zingsheim, H. P. & Oesterhelt, D. (1978). Recrystallization of the purple membrane *in vivo* and *in vitro*. *J. Mol. Biol.* **123**, 247–257.
 - Weinkauff, S. & Bachmann, L. (1992). Metal decoration of biomacromolecules and molecular assemblies: a review. *Ultramicroscopy*, **46**, 113–134.
 - Bacher, A., Weinkauff, S., Bachmann, L., Ritsert, K., Baumeister, W., Huber, R. & Ladenstein, R. (1992). Electron microscopy of decorated crystals for the determination of crystallographic rotation and translation parameters in large protein complexes. *J. Mol. Biol.* **225**, 1065–1073.
 - Meining, W., Bacher, A., Bachmann, L., Schmid, C., Weinkauff, S., Huber, R. & Nar, H. (1995). Elucidation of crystal packing by X-ray diffraction and freeze-etching electron microscopy. Preliminary structure analysis of GTP cyclohydrolase I. *J. Mol. Biol.* **253**, 208–218.
 - Braun, N., Tack, J., Fischer, M., Bacher, A., Bachmann, L. & Weinkauff, S. (2000). Electron microscopic observations on protein crystallization: adsorption layers, aggregates and crystal defects. *J. Cryst. Growth*, **212**, 270–282.
 - Pühler, G., Weinkauff, S., Bachmann, L., Müller, S., Engel, A., Hegerl, R. & Baumeister, W. (1992). Subunit stoichiometry and three-dimensional arrangement in proteasomes from *Thermoplasma acidophilum*. *EMBO J.* **11**, 1607–1616.
 - Gutman, A. & Hayek, K. (1980). Structural changes occurring during the separation of thin films of silver, copper, gold and nickel from their substrates. *Surface Tech.* **10**, 415–431.
 - Mårtensson, J. & Arwin, H. (1995). Interpretation of spectroscopic ellipsometry data on protein layers on gold including substrate-layer interactions. *Langmuir*, **11**, 963–968.
 - Arwin, H. (2001). Spectroscopic ellipsometry for characterisation and monitoring of organic layers. *Phys. Status Solidi sect. A*, **188**, 1331–1338.
 - Opila, R. L. & Eng, J., Jr (2002). Thin films and interfaces in microelectronics: composition and chemistry as function of depth. *Prog. Surf. Sci.* **69**, 125–163.
 - Ladenstein, R., Schneider, M., Huber, R., Bartunik, H.-D., Wilson, K., Schott, K. & Bacher, A. (1988). Heavy riboflavin synthase from *Bacillus subtilis*. Crystal structure analysis of the icosahedral (60 capsid at 3.3 Å resolution). *J. Mol. Biol.* **203**, 1045–1070.
 - Bacher, A., Ludwig, H. C., Schnepfle, H. & Ben-Shaul, Y. (1986). Heavy riboflavin synthase from *Bacillus subtilis*. Quaternary structure and reaggregation. *J. Mol. Biol.* **187**, 75–86.
 - Ladenstein, R., Ritsert, K., Huber, R., Richter, G. & Bacher, A. (1994). The lumazine synthase/riboflavin synthase complex of *Bacillus subtilis*. X-ray structure analysis of hollow reconstituted β-subunit capsids. *Eur. J. Biochem.* **223**, 1007–1017.
 - Ritsert, K., Huber, R., Turk, D., Ladenstein, R., Schmidt-Bäse, K. & Bacher, A. (1995). Studies on the lumazine synthase/riboflavin synthase complex of *Bacillus subtilis*: crystal structure analysis of reconstituted, icosahedral β-subunit capsids with bound substrate analogue inhibitor at 2.4 Å resolution. *J. Mol. Biol.* **253**, 151–167.
 - Löwe, J., Stock, D., Jap, B., Zwickl, P., Baumeister, W. & Huber, R. (1995). Crystal structure of the 20 S proteasome from the archaeon *T. acidophilum* at 3.4 Å resolution. *Science*, **268**, 533–539.
 - Schmid, C., Meining, W., Weinkauff, S., Bachmann, L., Ritz, H., Eberhardt, S. *et al.* (1993). Studies of Cyclohydrolase I of *Escherichia coli*. *Advan. Expr. Med. Biol.* **338**, 157–162.
 - Nar, H., Huber, R., Meining, W., Schmid, C., Weinkauff, S. & Bacher, A. (1995). Atomic structure of GTP cyclohydrolase I from *Escherichia coli*. *Structure*, **3**, 459–466.
 - Zeitler, E. & Bahr, G. F. (1965). Contrast and mass thickness. *Lab. Invest.* **14**, 946–954.
 - Bahr, G. F. & Zeitler, E. (1965). The determination of the dry mass in populations of isolated particles. *Lab. Invest.* **14**, 955–977.
 - Reimer, L. (1967). Deutung der Kontrastunterschiede von amorphen und kristallinen Objekten in der Elektronenmikroskopie. *Z. Angew. Phys.* **22**, 287–296.
 - Rübenkamm, E., Braun, N., Bachmann, L., Bacher, A., Brandt, J., Baumeister, W. & Weinkauff, S. (1995). Quantitative evaluation of heavy metal decoration on protein molecules. *Ultramicroscopy*, **58**, 337–351.
 - Ladenstein, R., Bacher, A. & Huber, R. (1987). Some observations of a correlation between the symmetry of large heavy-atom complexes and their binding sites on the proteins. *J. Mol. Biol.* **195**, 751–753.
 - Robins, J. L. & Rhodin, T. N. (1964). Nucleation of metal crystals. *Surf. Sci.* **2**, 346–355.
 - Braun, N., Tack, J., Bachmann, L. & Weinkauff, S. (1996). Orientation of globular proteins adsorbed on solid substrates: an electron microscopic analysis. *Thin Solid Films*, **284–285**, 703–707.
 - Schott, K., Ladenstein, R., König, A. & Bacher, A. (1990). The lumazine synthase/riboflavin synthase complex of *Bacillus subtilis*. Crystallization of reconstituted icosahedral β-subunit capsids. *J. Biol. Chem.* **265**, 12686–12689.
 - Weinkauff, S., Bacher, A., Baumeister, W., Ladenstein, R., Huber, R. & Bachmann, L. (1991). Correlation of metal decoration and topochemistry on protein surfaces. *J. Mol. Biol.* **221**, 637–645.
 - Bachmann, L., Weinkauff, S., Baumeister, W., Wildhaber, I. & Bacher, A. (1989). Electron microscopy of subnanometer surface features on metal decorated protein crystals. *J. Mol. Biol.* **207**, 575–584.
 - Saxton, O. & Baumeister, W. (1982). The correlation averaging of a regularly arranged bacterial cell envelope protein. *J. Microsc.* **127**, 127–138.
 - van Heel, M. (1984). Multivariate statistical classification of noisy images (randomly oriented biological macromolecules). *Ultramicroscopy*, **13**, 165–184.
 - Jones, A. T., Zan, J. Y., Cowtan, J. Y. & Kjeldgaard, M. (1991). Improved methods for building protein models in electron density maps and the location of errors in the model. *Acta Crystallog. Sect. A*, **47**, 110–119.

Edited by W. Baumeister

(Received 24 January 2002; received in revised form 14 June 2002; accepted 14 June 2002)